INTERNATIONAL JOURNAL OF OPTIMIZATION IN CIVIL ENGINEERING
Int. J. Optim. Civil Eng., 2012; 2(1):47-70

COMPOSITION OF ISOGEOMETRIC ANALYSIS WITH LEVEL SET METHOD FOR STRUCTURAL TOPOLOGY OPTIMIZATION

S. Shojaee[*, a,†], M. Mohamadian[b] and N. Valizadeh[a]
[a]*Department of Civil Engineering, Shahid Bahonar University, Kerman, Iran*
[b]*Civil Engineering Department, Ferdows Branch, Islamic Azad University, Ferdows, Iran*

ABSTRACT

In the present paper, an approach is proposed for structural topology optimization based on combination of Radial Basis Function (RBF) Level Set Method (LSM) with Isogeometric Analysis (IGA). The corresponding combined algorithm is detailed. First, in this approach, the discrete problem is formulated in Isogeometric Analysis framework. The objective function based on compliance of particular locations of materials in the structure is used and find the optimal distribution of material in the domain to minimize the compliance of the system under a volume constraint. The refinement is employed for construction of the physical mesh to be consistent with the mesh is used for level set function. Then a parameterized level set method with radial basis functions (RBFs) is used for structural topology optimization. Finally, several numerical examples are provided to confirm the validity of the method.

Received: 15 January 2012; Accepted: 30 March 2012

KEY WORDS: isogeometric analysis; topology optimization; shape optimization; level set method; radial basis functions

1. INTRODUCTION

An extensive development in structural shape and topology optimization has been experienced in recent three decades. Considerable researches and various topology optimization methods such as material distribution method [1-4], Solid Isotropic Material with Penalization (SIMP) methods [5-8], Bubble method [9] and Evolutionary Structural Optimization (ESO) method

[*]Corresponding author: S. Shojaee, Department of Civil Engineering, Shahid Bahonar University, Kerman, Iran
[†]E-mail address: saeed.shojaee@uk.ac.ir

[10] have been proposed. In recent years, the level set methods [11, 12] have been incorporated into structural shape and topology optimization field effectively. The major strength of level set method is that, it is an implicit method for moving interior and exterior boundaries and during the process; boundaries may join to each other.

Among the first researchers, Sethian and Wiegmann [13] extended the level set method in shape optimization. In their work, equivalent stress criteria update level set functions instead of solving equations. Osher and Santosa [14] also apply the level set method to the topology design problem of a two-density inhomogeneous drum membrane. In addition Allaire et al [15] and Wang et al [16] studied the structural topology optimization by combining the shape derivative [17-19] or sensitivity analysis with the level set model. Recently Wang et al [20] and Luo et al [21] have proposed Radial Basis Functions as a means to parametrize level set method. Shojaee and Mohamadian [22-24] have proposed binary and piecewise constant level set method and combined with a Merriman-Bence-Osher scheme to solve a structural shape and topology optimization problem.

There are generally two phases in the structural optimization process, the analysis phase and the boundary evolution phase. The first phase is usually performed with the finite element method (FEM). One drawback of FEM is that some approximation is involved in the geometrical definition of the boundaries of the problem domain. Furthermore, the imposition of the essential boundary conditions on the boundaries cannot be exactly accomplished. Also the adaptability and refinement of the solution in the FEM requires several communications between the discretized geometry and the analysis tool which is quite costly [25, 26].

Isogeometric Analysis (IGA) has been developed with the aim of integrating Non-Uniform Rational B-Splines (NURBS) based finite element analysis into the CAD. One main idea in developing isogeometric analysis has been to prevent time-consuming data conversion between CAD systems and the finite element analysis (FEA) in engineering problems. IGA is based on Non-Uniform Rational B-Splines (NURBS) basis function applied for both the solution field approximation and the geometry description. Therefore, CAD and FEA can be unified efficiently in one package. This leads to the ability of modeling complex geometries accurately. Moreover, simple and systematic refinement strategies, exact representation of common engineering shapes, robustness and superior accuracy can be achieved in comparison with the conventional finite element method. According to these features, isogeometric analysis is expected to become a powerful computational approach in the analysis of various engineering problems; as it has already been applied to structural problems, fluid mechanics, fluid-structure interaction, structural optimization [27-30]. Isogeometric shape optimization has been discussed by Cho et al. [31], Wall et al. [32], Nagy et al. [33], Qian [34], Seoa et al [35] and Shojaee et al [36] recently. The validity and efficiency of the approaches have been verified in a good manner.

The present paper proposes an integrated optimization approach based on the concept of isogeometric analysis and Radial Basis Function (RBF) level set method. The presented isogeometric analysis framework employs NURBS in the analysis stage. The optimization stage performs a RBF's based level set method to optimize topology. The isogeometric method is naturally associated with RBF level set method provides a very efficient treatment. In the following sections, a topology optimization problem is formulated based on the RBF level set method, and the method of isogeometric analysis is explained. The proposed topology

optimization method is applied to the minimum mean compliance problem. Finally, to confirm the validity and utility of the proposed topology optimization method, several numerical examples are provided.

2. LEVEL SET METHOD

The level set method is an implicit method for describing the evolution of an interface between two domains. It makes use of a function f, referred to as the level set function, which represents the boundary as the zero level set and nonzero in the domain [11, 12]. According to the value of the level set function:

$$\begin{cases} f(x(t)) > 0 & : \quad \forall x(t) \in D \setminus \Omega \\ f(x(t)) = 0 & : \quad \forall x(t) \in \partial\Omega \\ f(x(t)) < 0 & : \quad \forall x(t) \in \Omega \setminus \partial\Omega \end{cases} \tag{1}$$

where $D \subset R^d$ is a fixed domain in which all admissible form of Ω are included (i.e. $\Omega \subset D$). The level set function is used to define the inside and outside regions of interface. The boundary or interface is embedded as the zero level of the level set function. During the optimization process, the level set surface may move up and down, and this causes the embedded boundary to undergo drastic shape or topological changes. From beginning to end, the value of the level set function on the boundary is constantly kept to be zero

$$f(x) = 0.0 \quad , \forall x \in \partial\Omega \tag{2}$$

Differentiating in *t* yields,

$$\frac{\partial f}{\partial t} + \nabla f . v(x) = 0.0 \tag{3}$$

where $n(\mathrm{x}) = \frac{\mathrm{dx}}{\mathrm{dt}}$ is the velocity vector field, provided based on sensitivity analysis. Considering $n = \frac{\nabla f}{|\nabla f|}$ and $v.\nabla f = (v_n)|\nabla f|$, leads equation (3) takes the form,

$$\frac{\partial f}{\partial t} + v_n |\nabla f| = 0.0 \tag{4}$$

The solving procedure of equation (4) requires appropriate choice of the upwind schemes, reinitialization algorithm and extension velocity method, which may require excessive amount of computational efforts and thus limit the utility of the level set methods [11]. Therefore, a parameterized level set method with radial basis functions (RBFs) is used in the present study for structural topology optimization.

3. SHAPE AND TOPOLOGY OPTIMIZATION PROBLEM

3.1. Statement of optimization problem

The optimization goal is to minimize the compliance (global strain energy) over the structural domain with a constraint on total material volume resource. There exist numerous equivalent formulations of the minimum compliance problem that we use which was given in the work of Allaire et al. [15]. Let Ω be a smooth bounded open set, and is occupied by a linear isotropic elastic material with Hook's law A in design domain. A general objective function (compliance) can be formulated as,

$$J(\Omega)=\int_{\Omega} f.udv+\int_{\Gamma_N} g.uds=\int_{\Omega} Ae(u).e(u)dv \tag{5}$$

where Γ_N is Neumann boundary condition, f, g are body force and surface load respectively, and u is the displacement field based on the following linear elasticity equations

$$\begin{cases} -div(Ae(u))=f & in \quad \Omega \\ u=0 & on \quad \Gamma_D \\ (Ae(u))n=g & on \quad \Gamma_N \end{cases} \tag{6}$$

where Γ_D is Dirichlet boundary condition. The standard notion for minimum compliance design problems can be mathematically defined as follows

$$\begin{cases} Minimize\ J(\Omega)=\int_{\Omega} f.udv+\int_{\Gamma_N} g.uds=\int_{\Omega} Ae(u).e(u)dv \\ Subject\ to: \int_{\Omega} dv-V_{\max}\le 0 \end{cases} \tag{7}$$

3.2. Shape derivative

In order to apply a gradient method to the minimization of (7), we recall a classical notion of shape derivative. Murat and Simon [37] introduced a technique for constructing shape derivative by parameterization of domains. We use their approach as follows:

$$\Omega_q=(\Im+q)\Omega \tag{8}$$

Where Ω is a smooth open set domain, $\Im$ is identity mapping in $\Re^N$ and $q\in W^{1,\infty}(\Re^N,\Re^N)$. The shape derivative of objective function $J(\Omega): \Re^N \to \Re$ is defined as the Frechet derivative in $W^{1,\infty}(\Re^N,\Re^N)$,

$$J((\Im+q)\Omega)=J(\Omega)+J'(\Omega)q+O(q) \tag{9}$$

where $J'(\Omega)$ is a continuous linear form on $W^{1,\infty}(\Re^N,\Re^N)$ given as the unique solution to equation. 7. The sensitivity of the mean compliance (equation 7) is given as follows [15, 17],

$$J'(\Omega)q = \int_{\Gamma_N} (2[\frac{\partial(g.u)}{\partial n} + Hg.u + f.u] - Ae(u).e(u))q.nds + \int_{\Gamma_D} Ae(u).e(u)q.nds \quad (10)$$

where $H = divn$ is mean curvature, $\partial\Omega$ is the boundary of material domain. Ω can be decomposed as three parts, $\Gamma_D, \partial D_N, \Gamma_O$. Γ_D is admissible Dirichlet boundary conditions such that $\Gamma_D \subset \partial D_D$. $\Gamma_N = \partial D_N \cup \Gamma_O$ is Neumann boundary conditions where ∂D_N supports a non-homogeneous one and Γ_O supports homogeneous one. Let us suppose that there is no body force then in (5) $f = 0.0$, thus the objective function is defined as:

$$J(\Omega) = \int_{\partial D_N} g.uds \quad (11)$$

Therefore, the Frechet derivative of the mean compliance and the volume constraint can be reformulated as,

$$J'(\Omega)q = \int_{\Gamma_O} (-Ae(u).e(u))q.nds \quad (12)$$

$$V'(\Omega)q = \int_{\partial\Omega} q(x)n(x)ds \quad (13)$$

In order to solve the optimization problem, we use the augmented Lagrangian method. For a given penalty parameter (Λ^K) and Lagrange multiplier (l^K) the augmented problem can be stated as follows,

$$\bar{J}(\Omega) = J(\Omega) + l^K\left[\int_\Omega dv - V_{\max}\right] + \frac{1}{2\Lambda^K}\left[\int_\Omega dv - V_{\max}\right]^2 \quad (14)$$

The Lagrange multiplier and penalty parameters are updated as follows at each iteration of the optimization process,

$$l^{K+1} = l^K + \frac{1}{\Lambda^K}\left[\int_\Omega dv - V_{\max}\right] \quad (15)$$

$$\Lambda^{K+1} = a\Lambda^K \quad (16)$$

where $a \in (0,1)$ is a constant parameter. Using the shape derivative of equation (14) where there is no body force, gives,

$$\bar{J}'(\Omega)q = \int_{\Gamma_O} vq.nds \quad (17)$$

$$v = \left(l + \frac{1}{2\Lambda}\left[\int_{\Omega} dv - V_{\max}\right]^2 - Ae(u).e(u) \right) \tag{18}$$

To ensure the decrease of the objective function in level set method, the normal velocity field must be chosen appropriately. The fast descent or the steepest descent method is used such as proposed in Allaire et. al. [15] and Wang et. al.[16], which $q = -vn$. The normal velocity field in equation (4) is substituted with normal component of this direction $q.\boldsymbol{n} = -\boldsymbol{v}$.

$$\frac{\partial \Phi}{\partial t} - v\left|\nabla \Phi\right| = 0 \tag{19}$$

3.3. The RBFs based level set method

The use of explicit schemes for solving level set equation requires appropriate choice of the upwind schemes, reinitialization algorithms and extension velocity methods, which limit the application of the standard level set method to shape and topology optimization problems. For the sake of overcoming these drawbacks while retain the topological benefits of the implicit representation, we apply the Radial Basis Functions (RBFs) to represent the implicit level set modeling to reconstruct the shape and topology of an admissible design in a parametric way [16,20]. By using of this scheme, the original Partial Differential Equation (PDE) based level set method converts into a set of much easier Ordinary Differential Equation (ODE) system and makes the level set method more efficient to implement.

3.3.1. RBFs implicit modeling

Radial basis functions are used to approximate an admissible design with a single function which is globally continuous and differentiable. RBFs are radially-symmetric functions centered at particular points which can be expressed as,

$$j\,(x) = j\,(\left\|x - x_i\right\|),\ \ x_i \in D \tag{20}$$

Where $j : R^+ \to R$ with $j\,(0) \geq 0$ and x_i is the position of the point or the knot. There are a large number of different radial basis functions which can be roughly divided into two classes. One of these is the globally supported radial basis functions (GSRBFs) such as: thin-plate spline, Sobolev splines, polyharmonic splines, multiquadrics (MQ), inverse multiquadrics (IMQ) [39] and so on. The other is the compactly supported radial basis functions (CSRBFs) which is presented by Wendland [40]. In this paper the CSRBF with C2 continuity is chosen due to its strictly positive definiteness and the sparsity of collection matrices. The CSRBF C2 kernel (Figure 1-a) is defined as,

$$j_{\,i}(r) = \left(\max(0,(1-r))^4\right).(4r+1) \tag{21}$$

where the radius of support r is given in two dimension Euclidean spaces as

$$r = \frac{\sqrt{(x-x_i)^2 + (y-y_i)^2}}{d_{sp}} \tag{22}$$

where d_{sp} usually set large enough to guarantee there are enough knots located in the neighborhood of the current knot [39,40].

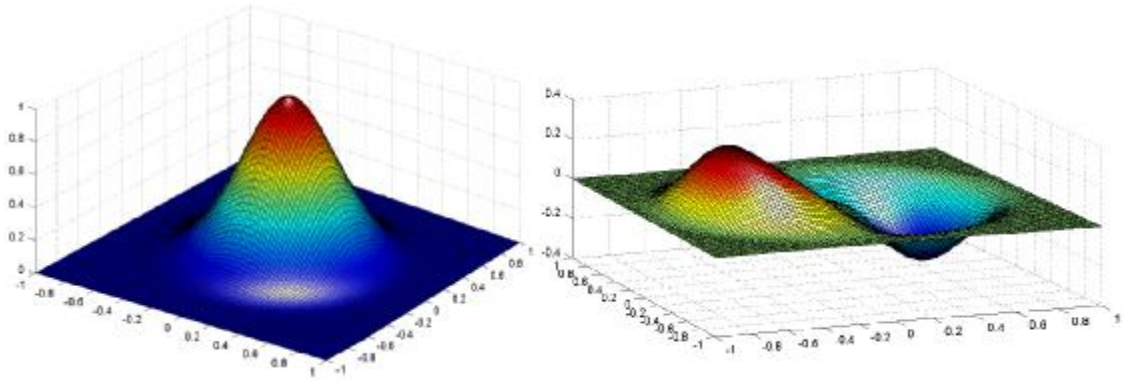

Figure 1. C2-CSRBF and its partial derivative in x direction

The derivatives of these CSRBFs can be easily obtained by the chain rule,

$$\begin{aligned} \frac{\partial j(x,y)}{\partial x} &= (\max(0,1-r))^3.(-20r).\frac{\partial r}{\partial x} \\ \frac{\partial j(x,y)}{\partial y} &= (\max(0,1-r))^3.(-20r).\frac{\partial r}{\partial y} \end{aligned} \tag{23}$$

where

$$\begin{aligned} \frac{\partial r}{\partial x} &= \frac{x-x_i}{d_{sp}.\sqrt{(x-x_i)^2 + (y-y_i)^2}} \\ \frac{\partial r}{\partial y} &= \frac{y-y_i}{d_{sp}.\sqrt{(x-x_i)^2 + (y-y_i)^2}} \end{aligned} \tag{24}$$

The implicit level set function $f(x)$ can be approximated with radial basis function

$$f(x) = \sum_{i=1}^{N} a_i j_i(x) = j^T(x)a \tag{25}$$

where a_i is the weight, which is usually called expansion coefficient.

3.3.2. RBF-level set optimization method

As aforementioned, we use RBF-level set method to transform the level set PDE equation into

a system of first-order ordinary differential equation (ODE). In this paper the RBF implicit modeling is used to approximate $f(x)$ by using CSRBF centered at knots,

$$f = f(x,t) = j^T(x)a(t) \tag{26}$$

With this parameterization the space and time become separate. Since the present RBF based interpolation scheme is performed under assumption that all the knots are fixed in the design domain thus, unlike the conventional discrete level set approach in the RBFs based parametric way, the design variables are the expansion coefficients a . Using equation (26) and equation (4) obtain,

$$j^T \frac{da}{dt} + V_n \left| \nabla j^T a \right| = 0 \tag{27}$$

To determine *n* unknown coefficient, one can use the collocation method and obtain a system of ODEs as follow

$$H \frac{da}{dt} + B(a) = 0 \tag{28}$$

Equation (28) can be solved by several different ODE solvers such as the first-order forward Euler's method and higher-order Runge-Kutta, Rung-Kutta-Fehlberg, Adames-Bashforth or Adams-Moulton method. In the present study the forward Euler method is used and an approximate solution to equation (28) can be given by

$$a(t_{n+1}) = a(t_n) + \Delta t H^{-1} B(a(t_n)) \tag{29}$$

where Δt is the time step. After obtaining the approximate solution in equation (29) at each time step, the level set function can be updated using equation (25).

4. ISOGEOMETRIC ANALYSIS

The traditional Finite Element formulations are based on interpolation schemes with Lagrange, Legendre or Hermite polynomials to approximate geometry, physical field and its derivatives. This approach often requires a substantial simplification of the geometry, particularly for curved boundaries of the analysis domain. Generally, adaptive refinement of the discretized domain is applied to better approximate the boundary and to achieve sufficient convergence. The concept of isogeometric analysis has been proposed by Hughes and coworkers recently [25]. The main idea of the isogeometric analysis is to apply the same interpolation scheme that is used accurately to describe the geometry for the approximation of the physical variables. Since NURBS basis functions have become standard basis for describing and modeling the geometry in CAD and computer graphics, they are used for describing both geometry and solution spaces.

4.1. B-spline and NURBS basis function

NURBS are a generalization of piecewise polynomial B-splines curves. The B-spline basis functions are defined in parametric space on a knot vector Ξ. A knot vector in one dimension is a non-decreasing sequence of real numbers:

$$\Xi = \{x_1, x_2, ..., x_{n+p+1}\} \tag{30}$$

Where x_i is the i^{th} knot, i is the knot index, $i = 1, 2, ..., n+p+1$, p is the order of the B-spline, and n is the number of basis functions. The half open interval $[x_i, x_{i+1})$ is called the i^{th} knot span and it can have zero length since knots may be repeated more than one, and the interval $[x_1, x_{n+p+1}]$ is called a patch. In the isogeometric analysis, always open knot vectors are employed. A knot vector is said to be open if it has $p+1$ repeating knots at the two ends.

With a certain knot span, the B-spline basis functions are defined recursively as,

$$N_{i,0}(x) = \begin{cases} 1 & \text{if } x_i \le x \le x_{i+1} \\ 0 & \text{otherwise} \end{cases} \tag{31}$$

and

$$N_{i,p}(x) = \frac{x - x_i}{x_{i+p} - x_i} N_{i,p-1}(x) + \frac{x_{i+p+1} - x}{x_{i+p+1} - x_{i+1}} N_{i+1,p-1}(x), \quad \text{p} = 1,\ 2,\ 3,\ \ldots . \tag{32}$$

A B-spline curve of order p is defined by

$$C(x) = \sum_{i=1}^{n} N_{i,p}(x) P_i. \tag{33}$$

where $N_{i,p}(x)$ is the i^{th} B-spline basis function of order p and P are control points, given in d-dimensional space ^{d}. 1-D B-splines basis functions, that are built from open knot vectors, are interpolatory at the ends of parametric space. Figure 2 shows the quadratic B-spline basis functions. In two dimensions, B-spline basis functions are interpolatory at the corners of the patches. The non-uniform rational B-spline (NURBS) curve of order p is defined as,

$$C(x) = \sum_{i=1}^{n} R_{i,p}(x) P_i \tag{34}$$

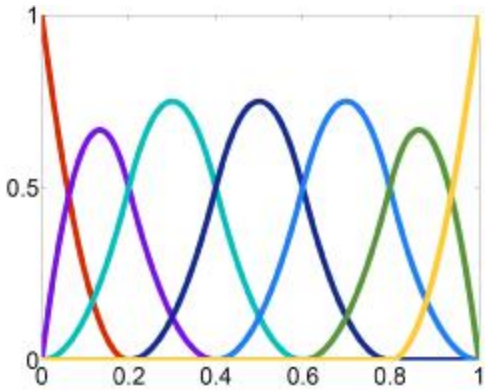

Figure 2. Quadratic basis functions for an open knot vector

$$\Xi=\{0,0,0,0.2,0.4,0.6,0.8,1,1,1\}$$

$$R_{i,p}(x)=\frac{N_{i,p}(x)w_i}{\sum_{i=1}^{n}N_{i,p}(x)w_i} \tag{35}$$

Here $R_{i,p}$ is the NURBS basis functions, P_i is the control point and w_i is the i^{th} weight that must be non-negative. In the two dimensional parametric space $[0,1]^2$, NURBS surfaces are constructed by tensor product through knot vectors $\Xi=\{x_1,x_2,...,x_{n+p+1}\}$ and $\Psi=\{y_1,y_2,...,y_{m+q+1}\}$. It yields to,

$$S(x,y)=\sum_{i=1}^{n}\sum_{j=1}^{m}R_{i,j}^{p,q}(x,y)P_{i,j} \tag{36}$$

where $P_{i,j}$ is the (i,j)-th of $n\times m$ control points, also called the control mesh. The interval $[x_1,x_{n+p+1}]\times[y_1,y_{m+q+1}]$ is a patch and $[x_i,x_{i+1})\times[y_j,y_{j+1})$ is a knot span. $R_{i,j}^{p,q}(x,h)$ is the NURBS basis function in two dimensional space,

$$R_{i,j}^{p,q}(x,y)=\frac{N_{i,p}(x)M_{j,q}(y)w_{i,j}}{W_{i,j}(x,y)} \tag{37}$$

and

$$W_{i,j}(x,y)=\sum_{i=1}^{n}\sum_{j=1}^{m}N_{i,p}(x)M_{j,q}(y)w_{i,j} \tag{38}$$

The derivative of $R_{i,j}^{p,q}(x,h)$ and $W_{i,j}(x,y)$ with respect to x is derived by simply

applying the quotient rule to (37) and (38),

$$\frac{\partial R_{i,j}^{p,q}(x,y)}{\partial x}=\frac{N'_{i,p}(x)M_{j,q}(y)w_{i,j}W_{i,j}(x,y)-\frac{\partial W_{i,j}(x,y)}{\partial x}N_{i,p}(x)M_{j,q}(y)w_{i,j}}{(W_{i,j}(x,y))^2} \tag{39}$$

and

$$\frac{\partial W_{i,j}(x,y)}{\partial x}=\sum_{i=1}^{n}\sum_{j=1}^{m}N'_{i,p}(x)M_{j,q}w_{i,j} \tag{40}$$

The domain of problem is divided into patches and each patch is divided into knot spans or elements. Patches play the role of sub-domains within which element types and material models are assumed to be uniform [25]. Nevertheless, many complicated domains can be represented by a single patch.

4.2. NURBS based isogeometric analysis formulation

Considering a 2-D linear elasticity problem with the presence of body force $\mathbf{b}$ and traction force $\bar{\mathbf{t}}$. Implementing the virtual displacement method, the following weak form equation is obtained,

$$\int_{\Omega}d\boldsymbol{\varepsilon}^T\boldsymbol{\sigma}d\Omega-\int_{\Omega}d\mathbf{u}^T\mathbf{b}d\Omega-\int_{\Gamma_t}d\mathbf{u}^T\bar{\mathbf{t}}d\Gamma=0 \tag{41}$$

where $\boldsymbol{\sigma}$ is the stress tensor and $\boldsymbol{\varepsilon}$ is the strain tensor. In isogeometric approach, the discretization is based on NURBS. Hence, the geometry and solution field are approximated as,

$$\mathbf{x}(x,h)=\mathbf{RP}\qquad x,h\in\Omega_{patch} \tag{42}$$

$$\mathbf{u}^h(x,h)=\mathbf{Rd}\qquad x,h\in\Omega_{patch} \tag{43}$$

where $\Omega_{patch}=\left\{(x,h)\middle|x\in\left[x_1,x_{n+p+1}\right],h\in\left[h_1,h_{m+q+1}\right]\right\}$. The matrix-form of $\mathbf{R}_{i,j}$ and $\mathbf{P}_{i,j}$ can be changed into vector-form by mapping from i, j subscripts to k by:

$$k=i+(j-1)n,\qquad \text{with } k=1,2,...,n.m \tag{44}$$

So, the control points are defined as,

$$\mathbf{P}=(\mathbf{P}_{1,1}{}^x,\mathbf{P}_{1,1}{}^y,\mathbf{P}_{2,1}{}^x,\mathbf{P}_{2,1}{}^y,...,\mathbf{P}_{n,m}{}^y)^T \tag{45}$$

The values of solution field at the control points, also called control variables, in the present IGA formulation are displacements and can be arranged similar to the control points in a

vector-form,

$$\mathbf{d} = (\mathbf{d}_{1,1}{}^{x}, \mathbf{d}_{1,1}{}^{y}, \mathbf{d}_{2,1}{}^{x}, \mathbf{d}_{2,1}{}^{y}, ..., \mathbf{d}_{n,m}{}^{y})^{T} \tag{46}$$

The matrix $\mathbf{R}$ is obtained from NURBS basis functions,

$$\mathbf{R} = \begin{bmatrix} R_{1,1} & 0 & R_{2,1} & 0 & ... & R_{n,m} & 0 \\ 0 & R_{1,1} & 0 & R_{2,1} & ... & 0 & R_{n,m} \end{bmatrix} \tag{47}$$

Next, the stiffness matrix for a single patch is computed as,

$$\mathbf{K}_{patch} = t \iint_{\hat{\Omega}} \mathbf{B}^{T}(x,h)\mathbf{D}\mathbf{B}(x,h)\left|\mathbf{J}\right| d\hat{\Omega} \tag{48}$$

where t is the thickness, $\hat{\Omega}$ is the parametric space, $\mathbf{B}(x,h)$ is the strain-displacement matrix, and $\mathbf{J}$ is the jacobian matrix which maps the parametric space to the physical space. $\mathbf{D}$ is the elastic material property matrix for plane stress. The force vector on a single patch in the presence of body forces $\mathbf{b}$ and traction forces $\bar{\mathbf{t}}$ is obtained as,

$$\mathbf{f} = \iint_{\hat{\Omega}} \mathbf{R}^{T}\mathbf{b}\left|\mathbf{J}\right| d\hat{\Omega} + \int_{\hat{\Gamma}} \mathbf{R}_{b}^{T}\bar{\mathbf{t}}\left|\mathbf{J}_{b}\right| d\hat{\Gamma} \tag{49}$$

where $\hat{\Gamma}$ is the traction boundary in the parametric space, $\mathbf{R}_{b}$ is the NURBS basis function evaluated on the traction boundary and $\mathbf{J}_{b}$ is the Jacobian that maps the traction boundary into a part of physical space boundary. The control variables can then be solved by the following discretized equilibrium equation,

$$\mathbf{K}\mathbf{d} = \mathbf{f} \tag{50}$$

The solution field at each point of the physical space can be approximated by equation (50). For numerical integration, the standard Gauss-quadrature is used over each element (knot span). The number of quadrature points depends on the NURBS order. The details of spaces, mapping and integration in isogeometric analysis are shown in Figure 3. Note that the physical mesh is only an image of knot spans on the physical space.

4.3. H-refinement or knot insertion

There are three types of refinement in isogeometric analysis: h-refinement or knot insertion, p-refinement or order elevation and k-refinement [25]. In this paper, we employed only the h-refinement.

Knot insertion is a procedure that arbitrary new knots are added to a knot vector without any change in the shape of the B-spline curve. If there are $m=n+p+1$ knots in the knot vector of the B-spline curve, where n is the number of control points and p is the order of B-spline

curve, by adding a new knot, a new control point must be added. Also, some current control points must be redefined. Consider a knot vector $\Xi = \{x_1, x_2, ..., x_{m=n+p+1}\}$ with n control points $P_1, P_2, ..., P_n$ and the order of p. Let $\hat{x} \in [x_k, x_{k+1}]$ be a desired new knot. The knot insertion procedure has the following 3 steps [31],

1. Find k such that $\hat{x}$ belongs to $[x_k, x_{k+1}]$.
2. Find $p+1$ control points $P_{k-p}, P_{k-p+1}, ..., P_k$.
3. Compute p new control points Q_i from the above $p+1$ control points using equation (27).

$$Q_i = (1-a_i)P_{i-1} + a_i P_i \tag{51}$$

where a_i is obtained from,

$$a_i = \frac{\hat{x} - x_i}{x_{i+p} - x_i} \quad \text{for} \quad k-p+1 \le i \le k \tag{52}$$

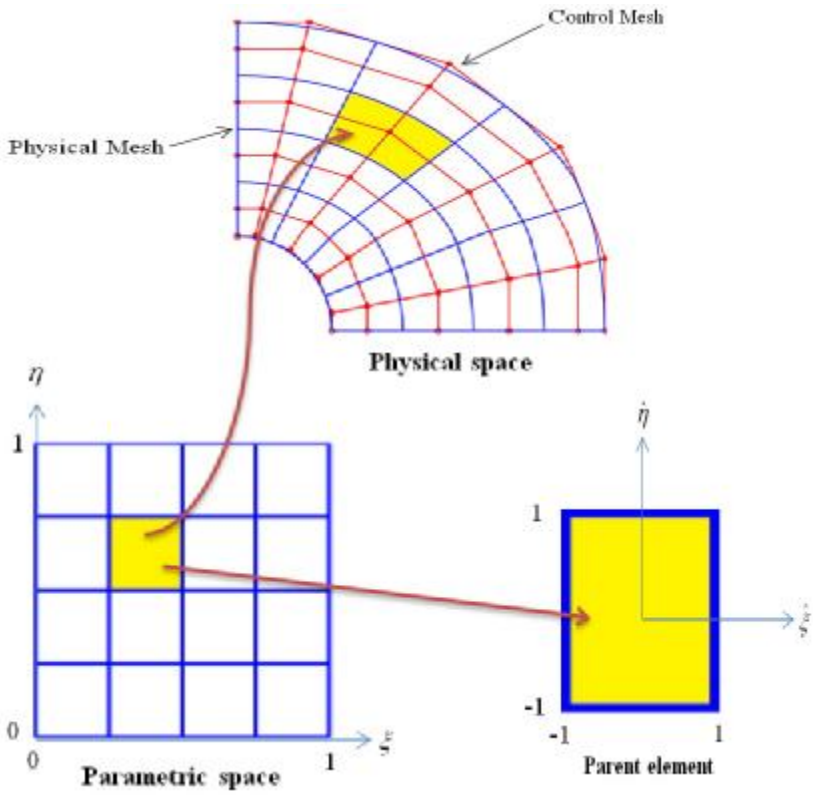

Figure 3. Physical space Ω is mapped into the parametric space $\tilde{\Omega}$ using NURBS basis functions. For numerical integration in the parametric space, each knot span is mapped to the parent element, where the integration is performed on

By performing the above procedure, the new knot vector and control points are obtained as,

$$\begin{gathered}\left\{x_1, x_2, ..., x_k, \hat{x}, x_{k+1}, ..., x_m\right\} \\ \left\{P_1, P_2, ..., P_{k-p}, Q_{k-p+1}, Q_{k-p+2}, ..., Q_k, P_k, P_{k+1}, ..., P_n\right\}\end{gathered} \tag{53}$$

Now, this knot insertion algorithm is extended to a NURBS curve. For this purpose, a given NURBS curve in d-dimensional space is converted into a B-spline curve in (d+1)-dimensional space, then by applying the knot insertion algorithm in this B-spline curve, the new control points are obtained. These new control points should then be projected to d-dimensional space to obtain the new control points of the NURBS curve. Consider control points $P_i = (x_i, y_i)$ with the weights w_i. By converting these control points to 3-dimensional space, $P_i^w = (w_i x_i, w_i y_i, w_i)$, the new control points are then computed from equation (27),

$$Q_i^w = (1 - a_i) P_{i-1}^w + a_i P_i^w \tag{54}$$

The location of control points in 2D are obtained by the following projection technique:

$$Q_i = \frac{(1 - a_i) P_{i-1}^w + a_i P_i^w}{(1 - a_i) w_{i-1} + a_i w_i} \tag{55}$$

and the weights are:

$$w_{Q_i} = (1 - a_i) w_{i-1} + a_i w_i \tag{56}$$

5. ISOGEOMETRIC ANALYSIS WITH LEVEL SET METHOD FOR STRUCTURAL TOPOLOGY OPTIMIZATION

In proposed approach, the discrete problem is formulated in isogeometric analysis framework. The general optimization problem stated in (5) is specified for an isogeometric discretization. We apply objective functions based on compliance of particular locations of the structure.

In geometry construction, we construct the geometry by performing knot insertion algorithm on the initial geometry model is shown in Figure 4. The initial geometry is modeled as a NURBS surface of bi-quadratic order with 6×4 control points. The open knot vectors in x direction is {0,0,0,0.25,0.5,0.75,1,1,1} and in y direction is {0,0,0,0.5,1,1,1}, which yields 4×2 knot spans. By dividing each knot span in x and y direction into 10 equal parts, the physical mesh with 40×20 equal knot spans and the control mesh with 42×22 control points is obtained that is shown in figure 5. Note that the location of the control points in the initial geometry model plays an important role in reaching the desired analysis model. We used the local support property of NURBS basis function, i.e., there are only $(p+1)\times(q+1)$ number of nonzero basis functions within each knot span, where p and q are the orders of NURBS. We know that each NURBS basis function has a corresponding control point. So, we can assign to each knot span, $(p+1)\times(q+1)$ control points. In this work, $p = q = 2$ and we have 3×3 control points for each knot span, as shown in Figure 5.

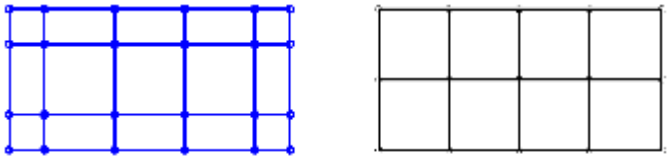

Figure 4. Initial geometry model. (a) Control mesh. (b) Physical mesh

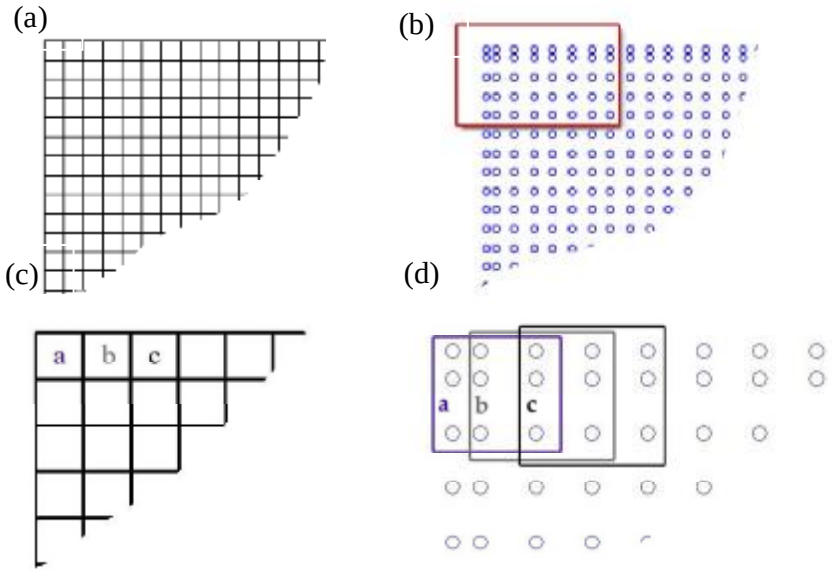

Figure 5. Geometry representation for the analysis model. (a) Physical mesh that is an image of 40×20 knot spans. (b) Control mesh that is consisting of 42×22 control points. (c) Local view of the left top corner of physical mesh, shows elements **a**, **b** and **c**. (d) Control points have supported on elements **a**, **b** and **c**

6. NUMERICAL IMPLEMENTATION

The objective of this section is to describe the numerical implementation of the proposed method. These implementations are developed to improve the performance of the proposed method.

6.1. Filtering

As mentioned before, shape derivative causes the level set function to have non- uniform value at points in design domain and can lead to numerical errors. To avoid quick changes and suppress the non smooth variation a filtering technique originally developed in image processing is used. One of the filtering approaches may be employed in structural topology optimization problems is convolution technique. In convolution based methods the density of each pixel is changed according to information from its neighborhood. The convolution

process can be formulated as,

$$\boldsymbol{c(i,j)=\sum_{k=1}^{n}\sum_{l=1}^{n}h(k,l)A(i+m-k,j+m-l)} \tag{57}$$

where $\boldsymbol{h(k,l)}$ is the density of the pixel located in the k^{th} row and l^{th} column of the image and $\boldsymbol{c}$ is the filtered density of the pixel. The so called impulse response matrix $\boldsymbol{A(i,j)}$ is a $\boldsymbol{n\times n}$ square matrix that has to be chosen according to the purpose of the filter. The variable $\boldsymbol{m=(n+1)/2}$, where n is the number of pixel in each side of the filter window. It should be noted that by implementing this method, the original optimization problem is changed and as result of seeking clear images, suboptimal results for the value of the objective function are obtained.

6.2. Ersatz material approach

A challenge to structural topology optimization is the fact that the isogeometric mesh will become distorted after the shape and topology change. Under these circumstances, the structure domain must be remeshed. However, remeshing is a complicating and time consuming task, and will bring down the efficiency of optimization. Instead, in this paper, the so-called "ersatz material" approach [15] which has been widely used in sensitivity analysis of the compliance optimization problem. In this approach the void domain is assumed to be replaced by a type of "weak" material, whose Young's modulus is very low. More precisely, we define a Young's modulus E_0 as,

$$E_0 = cE \tag{58}$$

Where E is the Young's modulus of the solid material of the structure and c is a coefficient.

The amount of this coefficient is selected as c = 1 for solid material and c = 0.0001 for void domain. Note that c cannot be too small, otherwise the stiffness matrix will be singular. Moreover, for the elements intersected by the boundary, Young's modulus is calculated according to the fraction of solid material. For example, in one element, if the volume of solid takes one half of the volume of the element, then the Young's modulus of this element is set to $E_0 = 0.5E$.

7. NUMERICAL EXAMPLES

In this section, two widely studied examples in structural topology optimization are used to illustrate the potentials of the proposed method. The optimization problem is considered as the compliance minimization subjected to volume constraint. The units of all the parameters can be defined flexibly, but they should remain unchanged during all different stages. All numerical examples have the following data, Young's modulus of real material is assumed 1, ersatz material $10^{-3,}$ Poisson' ratio for two material is assumed 0.3 and the order of NURBS basis functions in each direction is 2. In this method, the level set function is initially

embedded as a signed distance function, but no further reinitialization is applied in the rest of iterations. Also, the present algorithm is terminated when the relative difference between four successive objective function values is less than 10^{-4} or when the given maximum number of iterations has been reached.

7.1. Cantilever beam

Figure 6 shows the design domain of a cantilever beam with a size of $L=1$. The boundary of the left side is fixed, and a vertical concentrated force F=1N is applied at the center point of the right side boundary. The specified material volume fraction is 50%. In this example, we use Wendland C2-CSRBF and the knot points are distributed uniformly in the design domain.

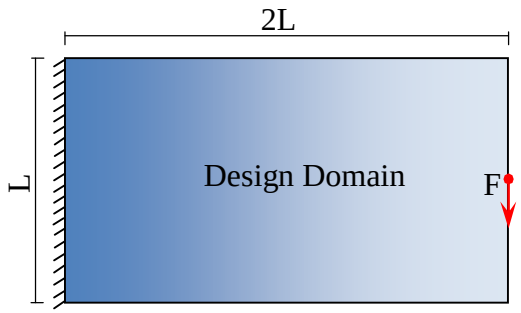

Figure 6. A cantilever beam

For comparison purpose, first, we apply finite element method as an analyzer when the level set mesh coincides with the finite element mesh. The design domain is discretized with 80×40 finite elements and the initial design is completely solid. It's clearly observed that the results of IGA by 800 elements agree well with FEA by 3200 elements. This IGA feature simplifies using of relatively coarse meshes in the topology optimization procedure.

Other parameters that are used for solving this example are ds=5, l =0, Λ = 20, a = 0.95. Figure 7 displays the evolution process of the cantilever beam at different stages. These figures show that the proposed level set method can handle shape fidelity and topological changes simultaneously by retaining a smooth boundary. In this method the initial level set surface is embedded as a signed distance function and we do not apply reinitialization at the rest of the topology optimization procedure. Also, because the Hamilton-Jacobi partial differential equation is converted to an ordinary differential equation, we do not need to meet the CFL condition for time step, thus we chose $t=10$ as a time step. These circumstances caused the nucleation of holes in design domain during the optimization process.

(a) Initial design (b) Step 10 (c) Step 15

(d) Step 20 (e) Step 25 (f) Final design

Figure 7. The evolution of optimal topology of the cantilever beam using FEA

Also, Figure 8 shows the strain energy and the volume fraction in different iterations.

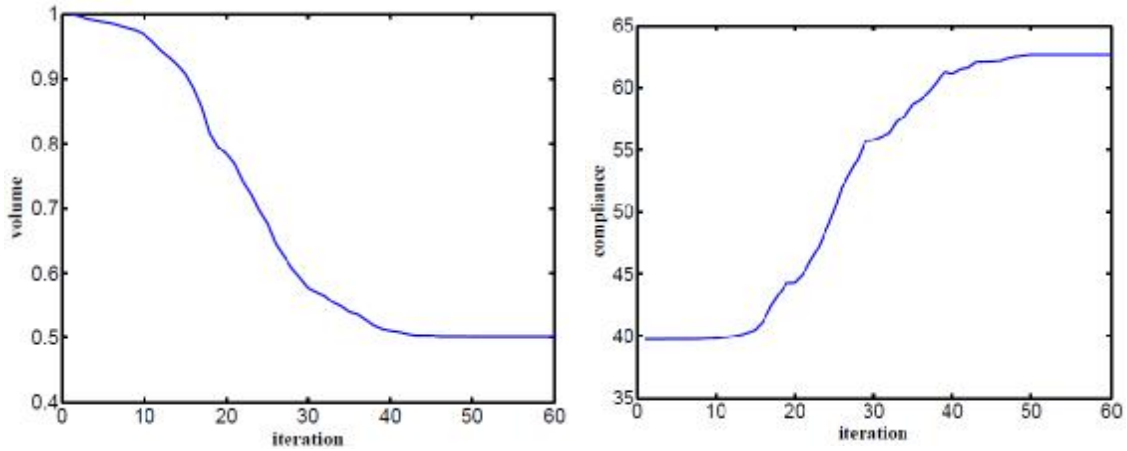

Figure 8. The History of objective function and volume

In second step, we optimized this example when the isogeometric analysis is applied. Here, the isogeometric mesh does not correspond with the level set mesh. More preciously, the design domain is divided with 40×80 level set mesh and 20×40 isogeometric mesh. The accuracy of the analysis when we apply isogeometric method with coarse mesh is partially the same as we use the finite element mesh with fine size. Figure 9 illustrate the designs in different stages of the optimization process, when we use the isogeometric method for analyzing. As shown in this figure, one can find that the two different schemes can lead to the similar designs. But, because in later scheme we use a coarse mesh for dividing the design domain, the total time of the optimization process when we apply the isogeometric method is much better than we use finite element method as an analyzer. The results obtained with the two different schemes are listed in Table 1. Figure 10 shows that the convergent curves of the objective function and the volume ratio.

(a) Initial design (b) Step 10 (c) Step 15

(d) Step 20 (e) Step 30 (f) Final design

Figure 9. The evolution of optimal topology of the cantilever beam using IGA

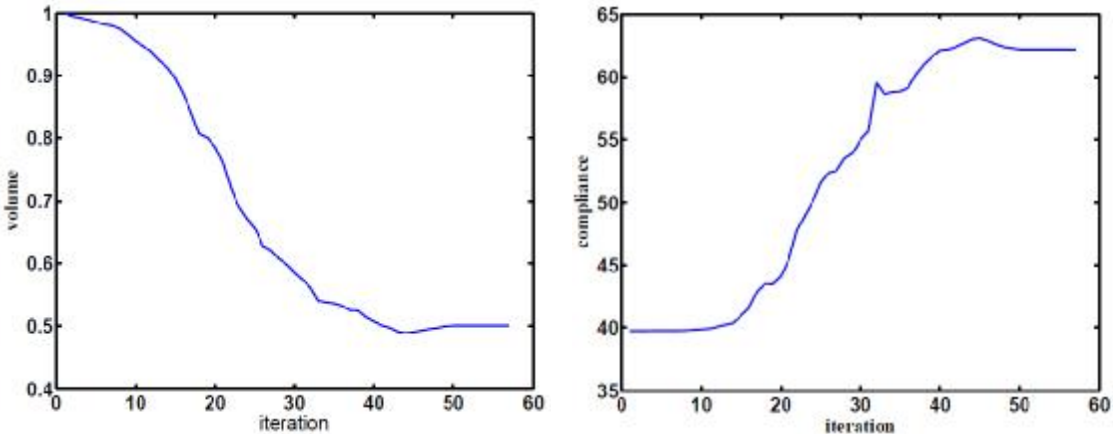

Figure 10. The History of objective function and volume ratio

Table 1. Comparison of the FEA and IGA

Analyzer	***J(Ω)* (objective)**	***T(s)* (total time)**	***N* (iterations)**
FEA	62.66	863.72	60
IGA	62.54	541.14	57

(a) With 12 holes

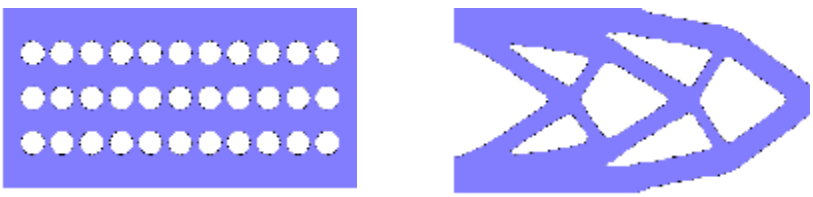

(b) With 33 holes

(c) With 44 holes

Figure 11. The effect of the initial design of the cantilever beam

We also investigate the influence of different number of initial holes on the final design. Figure 11 a, b and c show that the identical optimal structures are obtained regardless of number of initial holes in the design domain and the complexity of the final topologies do not change obviously with the different number of initial holes. In table 2 the results of these different initial designs are listed.

Table 2. Results of different designs of the cantilever beam

Initial design	***J(Ω)* (objective)**	***T(s)* (total time)**	***N* (iterations)**
Figure 13.a with 12 holes	63.06	531.02	53
Figure 13.b with 33 holes	62.83	536.55	55
Figure 13.c with 44 holes	62.88	537.63	55

7.2. A MBB beam

The design domain of a MBB beam is shown in Figure 12. A load F=300 is applied at the center of the top edge. Its left corner at the bottom is fixed and the right corner is supported as a roller. We also consider L=1 and the design domain is discretized with 120×30 elements. For this example, The IGA mesh is corresponding with level set mesh. The volume fraction is 40% and the other parameters, using for solving this problem, are $ds=5$, $l=0, \Lambda=30$, $a=0.9$. In Figure 13, the evolution of optimal topology is displayed by use of the present method.

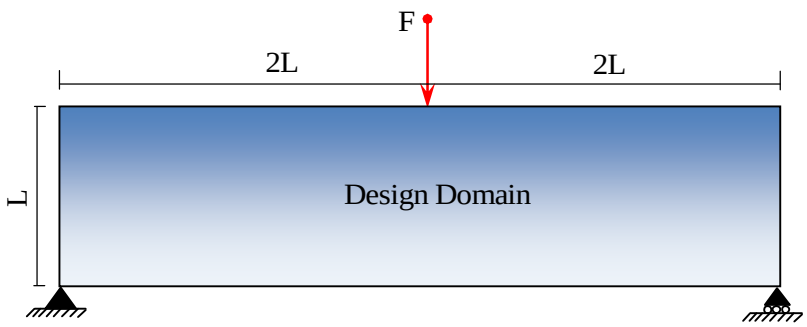

Figure 12. A MBB beam

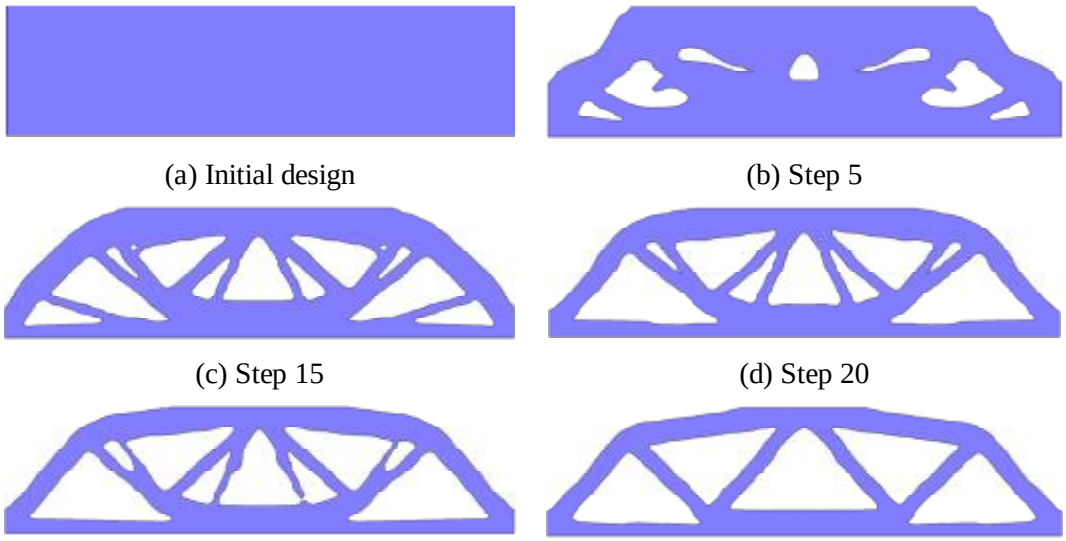

(a) Initial design (b) Step 5

(c) Step 15 (d) Step 20

(e) Step 25 (f) Final design

Figure 13. The evolution of optimal topology of the MBB beam

8. CONCLUSION

In the present study, the composition of RBF level set method with isogeometric analysis has been successfully applied to the structural shape and topology optimization. In this method, the discrete problem is formulated in isogeometric analysis framework. A parameterized level set method with RBFs is used for structural topology optimization. The proposed isogeometric based topology optimization method has several advantages compared to the finite element based method. Unlike the standard FEM-based design optimization, the computational time can be reduced by using this analyzer, while obtaining the same optimal topology. Due to the desirable characteristics of NURBS in IGA, it does not have any destructive effect on the quality of discretization. Furthermore, the proposed method in this paper has its strength on the capacity of dealing with the design dependent load problem or stress optimization problem.

REFERENCES

1. Allaire G, Kohn RV. Optimal bounds on the effective behavior of a mixture of two well-ordered elastic materials, *Quat Appl Math,* 1993; **51**: 643–74.
2. Allaire G, Bonnetier E, Francfort G, Jouve F. Shape optimization by the homogenization method, *Numer Math,* 1997; **76**: 27–68.
3. Suzuki K, Kikuchi N. A homogenization method for shape and topology optimization, *Comp Meth Appl Mech Eng,* 1991; **93**: 291–318.
4. Bendsøe M.P, Kikuchi N. Generating optimal topology in structural design using a homogenization method, *Comput Meth Appl Mech,* 1988; **71**(2): 197–224.
5. Bendsøe M.P, Optimal shape design as a material distribution problem, *Struct Optim,*

1989; **1**: 193–202.
6. Zhou M, Rozvany GIN. The COC algorithm, Part II: topological, geometry and generalized shape optimization, *Comput Meth Appl Mech*, 1991; **89**: 197–224.
7. Hassani B, Hinton E. A review of homogenization and topology optimization III-topology optimization using optimality criteria, *Comput Struct*, 1998; **69**: 739–56.
8. Bendsøe M.P, Sigmund O. *Topology Optimization: Theory, Methods, and Applications*, Springer, Berlin Heidelberg. 2003.
9. Eschenauer HA, Kobelev VV, Schumacher A. Bubble method for topology and shape optimization of structures, *Struct Optim*, 1993; **8**: 42–51.
10. Xie YM, Steven GP. A simple evolutionary procedure for structural optimization. *Comput Struct*, 1993; 885–96.
11. Osher S, Sethian J.A. Front propagating with curvature dependent speed: algorithms based on Hamilton–Jacobi formulations, *J Comput Phys*, 1988; **78**: 12–49.
12. Sethian J. Level set methods and fast marching methods: evolving interfaces in computational geometry, fluid mechanics, computer version and material science, Cambridge Monograph on Applied and Computational Mathematics, Cambridge University Press, UK. 1999.
13. Sethian JA, Wiegmann A. Structural boundary design via level set and immersed interface methods, *J Comput Phys*, 2000; **163**(2): 489–528.
14. Osher S, Santosa F. Level-set methods for optimization problem involving geometry and constraints: I. Frequencies of a two-density inhomogeneous drum, *J Comput Phys*, 2001; **171**: 272–88.
15. Allaire G, Jouve F, Toader A.M. Structural optimization using sensitivity analysis and a level-set method, *J Comput Phys*, 2004; **194**: 363–93.
16. Wang MY, Wang XM, Guo DM. A level set method for structural topology optimization, *Comput Meth Appl Mech*, 2003; **192**: 227–46.
17. Haug EJ, Choi KK, Komkov V. Design Sensitivity Analysis of Structural Systems, Academic Press, Orlando, 1986.
18. Sokolowski J, Zolesio JP. Introduction to Shape Optimization: Shape Sensitivity Analysis, Springer, Berlin, 1992.
19. Garreau S, Guillaume P, Masmoudi M. The topological asymptotic for PDE systems: the elasticity case. SIAM J. *Control Optim*, 2001; **39**(6): 175–78.
20. Wang SY, Wang MY. Radial basis functions and level set method for structural topology optimization. *Int J Numer Methods Eng*, 2006; **65**: 2060–90.
21. Luo Z, Tong LY, Kang Z. A level set method for structural shape and topology optimization using radial basis functions. *Comput Struct*, 2009; **87**: 425-34.
22. Shojaee S, Mohamadian M, A Binary Level Set Method for Structural Topology Optimization, *Int J Optim Civil Eng*, 2011; **1**(1): 73–90.
23. Mohamadian M, Shojaee S. Binary level set method for structural topology optimization with MBO type of projection, *Int J Numer Meth Engng*, 2012; **89**(5): 658–70.
24. Shojaee S, Mohamadian M. Piecewise constant level set method for structural topology optimization with Mbo type of projection, *Struct Multidisc Optim*, 2011; **44**(4): 455–69.
25. Hughes TJR, Cottrell J, Bazilevs Y. Isogeometric analysis: CAD, finite elements, NURBS, exact geometry and mesh refinement. *Comput Method Appl Mech*, 2005; **194**:

4135–95.
26. Cottrell J, Hughes TJR, Bazilevs Y. *Isogeometric Analysis: Toward Integration of CAD and FEA*, John Wiley & Sons, 2009.
27. Bazilevs Y, Beirao L, Veiga Da, Cottrell J, Hughes TJR, Sangalli G. Isogeometric analysis: approximation, stability and error estimates for h-refined meshes, **MATH** *Mod Meth Appl S*, 2006; **16**: 1031–90.
28. Cottrell J, Hughes TJR, Reali A. Studies of refinement and continuity in isogeometric structural analysis. *Comput Method Appl Mech*, 2007; **196**: 4160–83.
29. Bazilevs Y, Calo VM, Cottrell J, Evans J, Hughes TJR, Lipton S, Scott MA, and Sederberg T. Isogeometric analysis using T-splines. *Comput Method Appl Mech,* 2010; **199**(5–8): 229–63.
30. Hughes TJR, Reali A, Sangalli G. Efficient quadrature for NURBS-based isogeometric analysis. *Comput Method Appl Mech*, 2010; **199**: 301–13.
31. Cho S, Ha SH. Isogeometric shape design optimization: exact geometry and enhanced sensitivity, *Struct Multidiscip Optim*, 2009; **38**: 53–70.
32. Wall WA, Frenzel MA, Cyron C. Isogeometric structural shape optimization, *Comput Method Appl Mech*, 2008; **197**: 2976–88.
33. Nagy AP, Abdalla M, Gurdal Z. Isogeometric sizing and shape optimization of beam structures, *Comput Method Appl Mech*, 2010; **199**: 1216–30.
34. Qian X. Full analytical sensitivities in NURBS based isogeometric shape optimization, *Comput Method Appl Mech*, 2010; **199**: 2059–71.
35. Seoa Yu-Deok, Kima Hyun-Jung, Youn Sung-Kie. Shape optimization and its extension to topological design based on isogeometric analysis. *Int J Solids Struct*, 2010; **47**: 1618–40.
36. Shojaee S, Valizadeh N, Arjomand M. Isogeometric structural shape optimization using particle swarm algorithm, *Int J Optim Civil Eng*, 2011; **1**(4): 633–45.
37. Murat F, Simon S. Etudes de problems d'optimal design, *Lecture Notes in Computer Science*, 1976; vol. 41, Springer-Verlag, Berlin. 54–62.
38. Buhmann MD. *Radial Basis Function: Theory and Implementations*. Cambridge University Press, New York, NY. 2004.
39. Wendland H. Piecewise polynomial, positive definite and compactly supported radial functions of minimal degree. *Adv Comput Math*, 1995; **4**(1): 389–96.
40. Wendland H. Computational aspects of radial basis function approximation.In: Jetter K et al., editors. *Topics in Multivariate Approximation and Interpolation*, vols. 231–256. Elsevier BV, 2005.